



Accelerated Aging of Polymer Composite Bridge Materials

N. M. Carlson
L. G. Blackwood
L. L. Torres
J. G. Rodriguez
T. S. Yoder

March 1, 1999 – March 5, 1999

Smart Structures and Materials

This is a preprint of a paper intended for publication in a journal or proceedings. Since changes may be made before publication, this preprint should not be cited or reproduced without permission of the author.

This document was prepared as a account of work sponsored by an agency of the United States Government. Neither the United States Government nor any agency thereof, or any of their employees, makes any warranty, expressed or implied, or assumes any legal liability or responsibility for any third party's use, or the results of such use, of any information, apparatus, product or process disclosed in this report, or represents that its use by such third party would not infringe privately owned rights. The views expressed in this paper are not necessarily those of the U.S. Government or the sponsoring agency.



Accelerated aging of polymer composite bridge materials

N. M. Carlson,^a L. G. Blackwood, L. L. Torres, J. G. Rodriguez, and Timothy S. Yoder

Idaho National Engineering and Environmental Lab., P.O. Box 1625, Idaho Falls, ID 83415-2209

ABSTRACT

Accelerated aging research on samples of composite material and candidate ultraviolet (UV) protective coatings is determining the effects of six environmental factors on material durability. Candidate fastener materials are being evaluated to determine corrosion rates and crevice corrosion effects at load-bearing joints. This work supports field testing of a 30-ft long, 18-ft wide polymer matrix composite (PMC) bridge at the Idaho National Engineering and Environmental Laboratory (INEEL). Durability results and sensor data from tests with live loads provide information required for determining the cost/benefit measures to use in life-cycle planning, determining a maintenance strategy, establishing applicable inspection techniques, and establishing guidelines, standards, and acceptance criteria for PMC bridges for use in the transportation infrastructure.

Keywords: Durability testing, accelerated aging, PMC material, UV protective coating, composite bridge, analysis of variance, ANOVA

1. INTRODUCTION

The INEEL, in collaboration with the Federal Highway Administration, U.S. Department of Energy, Lockheed Martin Missile Advance Technology Center, Martin Marietta Materials, Idaho Transportation Department, University of Idaho, and Construction Technology Laboratories, Inc., is evaluating a 30-ft long, 18-ft wide PMC bridge. The performance of the bridge is being characterized with respect to design predictions and loads and evaluated with respect to safety and suitability for standard construction. Materials durability research is simulating environmental interactions in accelerated aging chambers to determine potential degradation mechanisms of the PMC, UV protective coating, and fasteners. Durability testing will provide both quantitative and qualitative data to assist engineers in the selection of fastener material, UV coatings, and fabrication practices for optimum life cycle performance of PMC bridges.¹

The PMC bridge, fabricated in 1994, was one of the first fiberglass reinforced polymer bridges and represents a simple support bridge in the 120-foot span category. After two years of evaluation, testing, and exposure to the mild, northern California environment, the bridge was disassembled in April 1997 and transported on a flat bed truck to the INEEL for field testing with live loads. The bridge was installed (in one day) in a prepared road site and instrumented with strain, deflection, and temperature sensors. As shown in Figure 1, the main axis of the bridge beams is oriented with the traffic flow. The deck plates and beams were bolted together, using Type 316 stainless steel bolts, without adhesive between the deck and beam flange to facilitate disassembly of the bridge at the conclusion of the tests. In a permanent installation, chemical bonding of the deck plates and beams would be desirable.

During the year and a half of field testing at the INEEL, dynamic and static load data have been acquired and analyzed.² The field test and interim aging results are summarized in this paper. Further information is available via the Internet.^b

2. INSTRUMENTED BRIDGE TESTING AND EVALUATION

Initial static testing in California showed that the bridge meet the primary length/800 maximum deflection requirements. Dynamic load data were required to further verify structural performance. At the INEEL, the bridge was instrumented to

a. Correspondence: Email: nmc2@inel.gov, Telephone: (208)526-6302, Fax: (208)526-0690

b. <http://www.inel.gov/capabilities/transportation/bridge1.html>

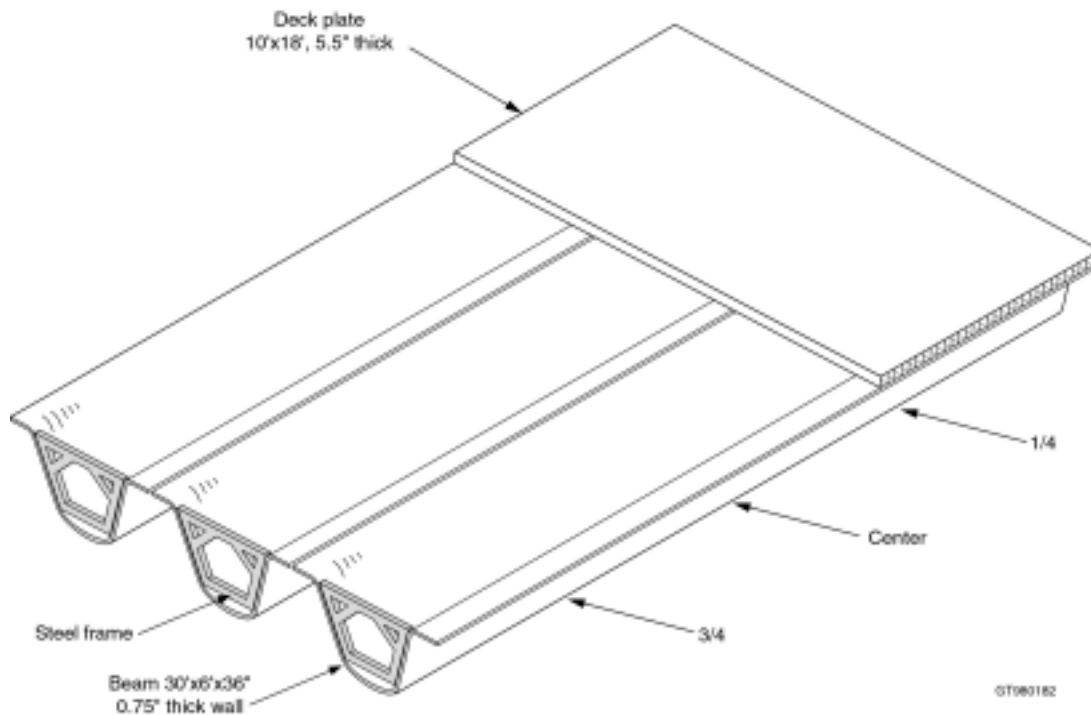


Figure 1. Schematic showing the three beams and one of the three deck plates. The beams have a quasi-isotropic wall of 56 oz. knitted fiberglass fabric $[0^\circ/45^\circ/90^\circ/-45^\circ]_8$ layup throughout beam, with a 0.95 in. buildup of 0° fiberglass reinforcement at the bottom (1.7 in. total thickness), and 0.96 HYDREX polyester-vinylester blend resin. Welded steel frames bolted inside the ends of the beams provide end rigidity. The deck plates' upper and lower face sheets are 56 oz. knitted fiberglass fabric with a $[0^\circ/45^\circ/90^\circ/-45^\circ/\text{mat}]_8$ layup using unsaturated polyester (2 plates) or vinylester (1 plate) resin. Their cobonded core is made from 18 ft. \times 4 in. \times 4 in. square pultruded tubes with C-channels at the ends for polymer-filled shear joints.

monitor strain (web, beam, deck, bolt), deflection (support, centerline, longitudinal, bridge length), longitudinal and transverse displacement during static and dynamic loading, temperature (wear surface, deck, beams), and environmental conditions (ambient temperature, humidity, solar radiation, ultra violet) at selected intervals. Sensor data are supplemented by frequent, detailed, visual inspections to evaluate the presence and extent of aging phenomena, such as abrasion of the deck wearing surface, impact/snow plow damage, connection integrity, and environmentally-induced deterioration that is not easily measured by sensors.

Loaded dump trucks and a loaded tractor belly dump trailer combination have been used in static load testing. The PMC bridge acts much like a steel or concrete bridge subject to similar conditions, loads, and restraint conditions. The biggest difference appears to be nonlinear elasticity of the bridge as it is loaded and unloaded. It may take more than 5 min for the bridge to rebound from the deflection caused by a static load. Temperature differences and restraint conditions have a significant impact on strain in the bridge. This is especially true for the bridge deck. Temperature differences may also have some impact on the modulus of elasticity of PMC.

3. DURABILITY TESTS

While the PMC bridge was under evaluation at the California test location, mechanical testing was performed on the PMC material. Areas identified for additional research were the durability of the UV coating as well as appropriate fastener material for the load bearing bolted joints holding the deck plate and beam together. The following sections discuss accelerated aging tests of the PMC and UV coating at the INEEL, freeze/thaw testing of PMC coupons, and accelerated aging of fasteners.

3.1 Accelerated Aging Of PMC and UV Coating

The tests are designed to simulate conditions the PMC and fasteners will experience during their life cycle. In addition, a weathering rack near the bridge is used to acquire weathering data on a smaller sample set. The accelerated aging tests are using 3 × 5 in. coupons of bridge beam material with and without UV protective coatings (tan gel coat, dark blue gel coat, tan urethane, and dark brown urethane—the bridge’s UV coating is tan gel coat). Two coating types were evaluated to establish performance of the lower cost gel coat relative to the more expensive urethane coating. For each coating type, both a light and dark color were evaluated to determine the effect of color on environmental interactions. To ensure that the coatings were applied as on the INEEL PMC bridge, the bridge fabricator, ACME Fiberglass, Inc., Hayward, CA., applied all UV coatings on test coupons at their facility using standard application processes. The initial test exposure simulated wind erosion, UV radiation, salt spray, rock hits from traffic, temperature cycling promoting condensation, and wet/dry cycling. The performance of four UV protective coatings and of uncoated coupons is evaluated using a full-factorial test matrix. Degradation is quantified by gloss and color measurements as well as by American Society for Testing and Materials (ASTM) standard visual tests for chalking. Additional visual inspection measures to establish cracking, blistering, checking, and flaking were evaluated and determined to provide no information on coating degradation during the testing cycle selected. Because ASTM standards have not been developed to specifically address the accelerated aging of UV coatings on composite materials, or of uncoated composite materials, for fabrication of bridges, we are using and adapting ASTM standards that have been developed for related applications.

Two accelerated aging test chambers provide carefully controlled test environments for cyclic accelerated aging—a Q-Panel QUV accelerated weathering tester provides the UV exposure and a Q-Fog Cyclic Corrosion Tester 1100 the salt spray exposure.³ The QUV accelerated weathering tester is designed to simulate moisture- and light-induced damaging effects of weathering. The QUV’s Solar Eye provides the desired UV irradiance. The Q-Fog Cyclic Corrosion Tester exposes specimens to a series of different environments in a repetitive cycle. These tests used the salt mist, dry-off, and humidity functions.

The QUV uses UVA-340 lamps to simulate sunlight, a condensation system to simulate rain and dew, and a spray system to simulate water erosion. UVA 340 lamps were chosen to simulate sunlight in the critical short wavelength UV region between 365 nm and solar cut off of 295 nm; the peak emission is at 340 nm. (UVA exposure is similar to sunlight exposure whereas exposure to the more aggressive UVB may not simulate natural weathering processes.) The QUV’s Solar Eye closed loop sensing and control system provides the desired UV irradiance, quick results without jeopardizing the correlation, and maximum UV for fast results. The QUV will also average low UV exposures. The QUV meets the requirements of ASTM G53-95⁴ using the parameters given in Table 1.

The Q-Fog Cyclic Corrosion Tester exposes specimens to a series of different environments in a repetitive cycle.⁵ These tests used the salt mist, dry-off, and humidity functions. The test solution that simulates salt spray is water containing 0.9% NaCl, 1% CaCl₂, and 0.25% NaHCO₃; the pH was between 6 and 8. The salt spray tests were performed in accordance with General Motors Engineering Standard GM9540, Method B, *Accelerated Corrosion Test*,⁶ using the parameters given in Table 2.

Table 1. QUV chamber parameters for UV radiation exposures.

Step	Conditions	Time
1	UV Exposure at 60°C using UVA-340 lamps (irradiance of 0.77 W/m ² /nm)	4 hours
2	Condensation (pure water) at 50°C (no UV)	4 hours

Table 2. Q-Fog chamber parameters for salt spray tests.

3	Conditions	Time
1	Subcycle Steps 2-3, repeat 4 times	—
2	Salt mist at 25°C	15 minutes
3	Dry-Off at 25°C	75 minutes
4	Dry-Off at 25°C	120 minutes
5	Humidity at 49°C (95 - 100 RH)	8 hours
6	Dry-Off at 60°C	7 hours
7	Dry-Off at 25°C	1 hour
8	Final Step - Go to step 1	—

Prior to QUV and Q-Fog exposure, some composite coupons were subjected to sandblasting, simulating wind erosion, and rock hits, simulating rock hits from traffic, to determine to their effects on a new UV protective coating and on the coating's performance during aging. Additional sandblasting and rock hits are planned on aged coupons because aged coatings may react differently to wind erosion and rock hits. The grit used for sandblasting represents air-borne debris and simulates INEEL dirt blown around in a windstorm. The calibrated rock hit exposure at 90° impact angle was performed by Q-Panel in Miami, Florida, according to ASTM D3170-87.⁷

Gloss measurements were taken with a BYK-Gardner micro-Tri-gloss reflectometer. This unit is designed to determine the gloss of paint coatings, plastics, ceramics, and similar materials by measuring reflected light and is capable of statistically evaluating a series of measurements. It meets ASTM D523-94.⁸ Gloss readings were acquired for angles of 65° and 80°. The gloss meter is calibrated prior to each use with a gloss standard for each acquired angle to verify equipment operation. The recorded gloss reading is the average value of four gloss readings acquired at set locations on each coupon.

Color measurements, taken with a Hunter Lab Miniscan XE spectrophotometer, were used to monitor changes in color intensity and brightness for each coupon. The color meter readings are verified using a reference color standard, a green tile with National Institute of Standards and Technology (NIST) traceable color values. Color meter readings were acquired in accordance with ASTM D2244-93⁹ using the Hunter Lab (L, a, b) scale, an illuminant of D₆₅ (noon daylight), and a 10° standard observer. The instrument has a diffuse/0° geometry with a small area of view (8 mm) and uses a NIST-traceable white tile standard and black light trap for calibration. Coupons were placed in a holder so that color measurements could be taken at the same location on each coupon with the port face down on the coupon; nine readings per coupon were averaged to obtain a color reading. Both the color and gloss meters are portable and easy to use in the field. (Readings are currently being acquired quarterly on the INEEL PMC bridge. One consideration in using the equipment in the winter months is extreme cold will effect the display feature so inspections must be done when temperatures are above freezing.)

3.1.1 Experimental Procedure

Prior to accelerated aging, composite coupons, with labels attached, were weighed and initial gloss and color measurements were acquired (following sandblasting and rock hits, if required). Then coupons were placed in the appropriate accelerated test chamber. The coupons were labeled by attaching a Teflon tag stamped with the coupon identification to the non-UV exposed side with silicon RTV. The coupons were not handled excessively. Coupons were rinsed with deionized water and mild detergent. They were handled with gloves after cleaning and care was taken to avoid contamination. Control coupons of each coating and of the uncoated composite, as well as of coupons that had been sandblasted or rock hit, were wrapped in white copy paper, held with rubber bands, and stored in the dark. The composite coupons were handled in accordance with ASTM G147-96, *Conditioning and Handling of Nonmetallic Materials for Natural and Artificial Weathering Tests*.¹⁰

Composite coupons were tested following GM9540, Method B⁶ and ASTM G53-95.⁴ Coupons were examined and repositioned weekly. To minimize effects from horizontal or vertical variations in UV exposure or temperature, coupons in the QUV that were located on the top of the bracket were moved to the lower slot. For the Q-Fog chamber, coupons next to the nozzle were moved away from the nozzle and those located in the outer areas were moved inwards. Each chambers' test duration was 2016 h (nominally 12 weeks). Coupons exposed to both Q-Fog and QUV chambers alternated between chambers on a weekly cycle in accordance with ASTM D5894-96¹¹; total time in each chamber was 12 weeks with the test duration of nominally 4000 hours.

Each week composite coupons were examined for chalking (ASTM D4214-89¹²), checking (ASTM D660-93¹³), cracking (ASTM D661-93¹⁴), blistering (ASTM D714-94¹⁵), and flaking (ASTM D772-86¹⁶) as well as evaluated with the gloss and color meter. If visual examination revealed changes between two cycles, photographs of the coupon were taken. After 2016 or 4000 hours of testing and visual examination, the coupons were weighted to determine weight change. Final color, gloss, and visual evaluations were made.

3.2 Statistical Analysis Method and Results

A multiple analysis of variance (ANOVA) was used to study the effects of five independent variables (coating type, rock hits, sandblasting, QUV exposure, and Q-Fog exposure) on the dependent variables (coupon weight, gloss, and color). All dependent variables were expressed in terms of change between the pretest and posttest measurements. A separate multiple ANOVA was performed for each dependent variable. In a multiple ANOVA, two types of statistical effects can be assessed,

main effects and interaction effects. A main effect is essentially the effect of a single independent variable averaged over all levels of the other variables (e.g., the effect of coating type averaged over all levels of sandblast, rock hit, QUV, and Q-Fog treatment). The main effects are analogous to the overall effect tested in a one-way ANOVA. An interaction effect occurs when the effect of a particular independent variable depends on the level of one or more of the other independent variables (e.g., the effect of rock hits may differ for coupons receiving QUV exposure as compared to those that do not). Interaction effects can be two-way (the effect of one variable depends on the level of one other variable), three-way (the effect of one variable depends on the combined levels of two other variables), etc. The basic analysis of variance table, indicating the types of interactions tested is given in Table 3.

Table 3. Analysis of variance.

	Effect	Degrees of Freedom
Main effects	Coating type (C)	4
	QUV (V), Q-Fog (F), Sand blast (S), Rock hit (R)	1
Two-way interaction effects	C*V, C*F, C*S, C*R	4
	V*F, V*S, V*R, F*S, F*R, S*R	1
Three-way interaction effects	C*V*F, C*V*S, C*V*R, C*F*S, C*F*R, C*S*R	4
	V*F*S, V*F*R, V*S*R, F*S*R	1
Four-way interactions	C*V*F*S, C*V*F*R, C*V*S*R, C*F*S*R	4
	V*F*S*R	1
Five-way interaction	C*V*F*S*R	4
Random error		50
Total		129

Note: The degrees of freedom specified are for use in computing F-tests for significance of effects once the data are collected and analyzed.

3.1.2.1 Weight Loss

While it was originally thought that coupons might gain weight due to the absorption of water, the trend was toward weight loss due to other aspects of the tests. The main effects for weight loss, except sandblast, were statistically significant. The sandblast effect was marginally significant as it appears the gel coat was tacky and had initially retained some of the sand blast material. Overall, the two urethane coatings performed similarly and showed the least weight loss. Tan gel coat coupons showed the greatest weight loss, exceeding even that for the uncoated coupons. Blue gel coat coupons performed about the same as the uncoated coupons. The mean weight loss values for QUV and Q-Fog treated coupons were approximately equal. Overall differences between rock hit and sandblasted coupons are quite small. However, these treatments should not be considered unimportant as they both contribute to significant interaction effects.

The five-way interaction between coating, QUV, Q-Fog, sandblast, and rock hit was statistically significant. The tan and brown urethane coupons are quite similar, but noticeably different from the gel coat coupons. Most notable in the mean weight loss values for the urethane coupons is the interaction between Q-Fog and QUV for sandblasted coupons. For these coupons, Q-Fog exposure increases weight loss for coupons not seeing QUV exposure but not for those exposed to QUV. This pattern is also evident in the brown urethane coupons with sandblast and rock hit exposure but not for any other urethane coupons.

The better performance of the urethane coatings vs. the gel coat coatings extends over almost all the treatment combinations involving QUV and Q-Fog exposure. In the absence of QUV or Q-Fog exposure sandblasting and rock hits had approximately the same effect on the gel coat and urethane coupons. Some of the uncoated coupons showed the largest effect of QUV exposure on weight loss.

3.1.2.2 Color

3.1.2.2.1 Color Mean *L*

In the Hunter **L,a,b** color scale, the **L** value measures light(100) to dark (0), **a** measures red (+**a**) to green (-**a**), and **b** measures yellow (+**b**) to blue (-**b**). Using the **L,a,b** scale, school bus yellow can be described as $L=69.7$, $a=12.7$, $b=60.5$. For the change in color mean **L**, the main effects for coating, QUV exposure, Q-Fog exposure and rock hit were statistically significant and the greatest effects are due to differences in coating and in Q-Fog exposure. All coatings types showed increases in color mean **L** values during testing as the result of chalking. The tan and brown urethane coatings experienced less chalking than the gel coatings and the tan gel coat performed better than the blue gel coat. The uncoated coupons showed color change between those for the two gel coatings. The overall effect of Q-Fog exposure was to produce a positive change in the color mean **L** value. Rock hits produced a small increase in color mean **L** while QUV exposure resulted in a small decrease.

There was also a significant four-way interaction effect between coating type, QUV exposure, Q-Fog exposure, and rock hits in the color mean **L** data. The role of rock hits in the four-way interaction is primarily observable in its effect on the uncoated samples. Rock hits increased the change observed in uncoated coupons—except for those seeing no QUV or Q-Fog exposure, which remained at about the same level with and without rock hits. For the other coating types, rock hits appears to have little effect regardless of QUV and Q-Fog exposure. Another interesting pattern in the four-way interaction data involves QUV and Q-Fog exposure. For coupons not receiving QUV exposure, Q-Fog exposure tends to produce relatively large increases in the color mean **L** value, possibly due to solution residue not removed using the ASTM cleaning procedure. However, for coupons that do receive QUV exposure, the effect of Q-Fog exposure is reduced. This effect is most noticeable for the blue gel coat coupons, but exists for other coatings as well. For the urethane coupons, applying both QUV and Q-Fog actually produced small negative changes in color mean **L**.

3.1.2.2.2 Color Mean *a*

All five treatment variables showed significant main effects on the change in color mean **a**. QUV exposure, sandblasting, and rock hits showed relatively small negative effects (i.e., a shift towards green) on the mean **a** value. Q-Fog showed a somewhat larger positive effect (shift towards red). The largest main effects occurred with coating type. Blue gel coat coupons showed a considerable shift toward green while uncoated coupons showed a shift towards red. The two urethane coatings showed small shifts towards green. The tan gel coat coupons showed essentially no change in mean **a** value.

While the main effects indicated that the biggest overall changes in color mean **a** occurred for blue gel coat coupons as compared to other coatings, the analysis indicates that the other coating types actually show changes of the same magnitude for certain treatment combinations. In particular, tan gel coat coupons receiving Q-Fog vs. no Q-Fog exposure showed large positive (green) shifts and large negative (red) shifts, respectively. Because these changes are in opposite directions, their effects averaged out to produce a near zero change in the overall mean plot for tan gel coat coupons. A similar pattern (but to a lesser degree) is observed for the uncoated coupons. The other coatings showed far less effects from Q-Fog. The data also show that the effect of sandblasting can be positive in some cases and negative in others in regard to color mean **a** shifts.

For color mean **a**, there was a significant interaction effect with coating type, QUV exposure, sandblasting, and rock hits. Also there were three significant three-way interaction effects not covered by the significant four-way interaction: the coating by QUV by Q-Fog interaction, the coating by Q-Fog by sandblast interaction, and the QUV by Q-Fog by sandblast interaction.

The three way interaction involving coating, QUV, and Q-Fog illustrates another way in which the various coating types respond differently to weathering effects. While tan gel coat coupons and uncoated coupons react similarly to Q-Fog exposure (i.e., color mean **a** increases with Q-Fog exposure), their responses to QUV exposure are in opposite directions. Color mean **a** decreases with QUV exposure for tan gel coat coupons but increases for the uncoated sample. The brown urethane coupons show little effect of either QUV or Q-Fog exposure.

3.1.2.2.3 Color Mean b

Overall, the blue gel coat and both urethane coatings showed little change in regard to absolute color mean **b** main effects. Tan gel coat coupons showed an appreciable negative shift (i.e., towards blue) while uncoated coupons shifted a similar distance in the positive direction (i.e., towards yellow). The overall effects of QUV exposure, Q-Fog exposure, and rock hits, while statistically significant, are small by comparison to coating types. The sandblast effect was not statistically significant.

A significant four-way interaction effect relative to changes in color mean **b** occurred among coating type, QUV, Q-Fog, and sandblast. Two-way interactions not covered by the four-way interactions were also significant (coating vs. rock hit and sandblast vs. rock hit). Analysis of data for the sandblast by rock hit interaction effect shows that the rock hit effect is to increase color mean **b**, and that the effect is greater for sandblasted coupons than for non-sandblasted coupons. The four-way interaction between coating type, QUV exposure, Q-Fog exposure, and sandblasting indicates that large changes in color mean **b** due to Q-Fog exposure are limited to tan gel coat and uncoated coupons. Within those coating types, the Q-Fog effect is greatest for non-QUV samples. For non-QUV tan gel coat coupons, Q-Fog exposure decreases color mean **b**. For non-QUV uncoated coupons the opposite effect occurs. Sandblasting seems to enhance the differences.

3.1.2.2.4 Color Summary

If a color measure of degradation is to be used for field inspection, information will need to be developed for specific coatings by color because degradation is manifested differently for each coating type and color. Use of mean **L** will provide quantitative records of the chalking process as the coating degrades and could be factored into a maintenance plan for coating repair.

3.1.2.3 Gloss

The only significant main effect indicated in the ANOVA for gloss retention was the main effect for sandblast exposure. However, further analysis of the individual means for the various coating types indicates that the gloss retention for the tan urethane is significantly higher than for the other coatings. (The lack of significant differences between the gloss retention values for the gel coated coupons, brown urethane coupons, and uncoated coupons led to the nonsignificance for the overall test of coating type.) Gloss retention for the tan urethane coupons was more than twice the combined median value for the other coating types.

The median gloss retention for sandblasted coupons was reduced to roughly 60% of the value for non-sandblasted coupons. The nonsignificant reduction in gloss retention for rock hit coupons was likely due to the fact that rock hits affect a much smaller percentage of the surface area than do the other treatments.

Although there were no significant main effects of QUV exposure, Q-Fog exposure, or rock hits, each of these variables occurs in the two significant interactions for the gloss ratio data. The two significant interactions were the QUV by Q-Fog effect and the coating by QUV by rock hit effect. The QUV by Q-Fog interaction shows that the effect of Q-Fog on the gloss ratio for sample coupons depends on whether or not the coupons also had QUV exposure. For coupons not receiving QUV exposure, the effect of Q-Fog is to decrease the gloss ratio. However, for coupons receiving QUV exposure, the effect of Q-Fog is to increase the gloss ratio. The coating by QUV by rock hit interaction indicates that the rock hit effect on gloss retention is primarily limited to the tan and brown urethane coated coupons. Furthermore, with the tan and brown urethane samples, the rock hit effect was limited to the coupons receiving QUV exposure. However, the effects were in the opposite direction between the coating types, i.e., the gloss ratio was reduced for the tan urethane QUV exposed coupons but was increased for the brown urethane QUV exposed coupons.

The measure of gloss is used to determine degradation of gel coat, with a nominal 50% reduction in gloss considered to be significant.¹⁷ Preliminary color and gloss durability results indicate the tan gel coat may be the least durable of the tested coatings. Discussions with the gel coat manufacturer revealed that the application of gel coat on the bridge, as well as the test coupons, was nonstandard as gel coat is not meant to be used as a post fabrication coating but rather the initial layer in a molding process. This nonstandard method of applying gel coat resulted in initially low gloss values as well as a tacky surface on both gel coat colors. Properly applied gel coat should be evaluated for environmental interactions to better judge its applicability to use in PMC bridge fabrication.

3.2 Freeze/Thaw Testing OF PMC and Coatings

Ten samples were tested in accordance with ASTM C666-92, “Standard Test Method for Resistance of Concrete to Rapid Freezing and Thawing (Procedure A-Freezing and Thawing in Water).” Construction Technology Laboratories of Skokie, IL performed tests, as the INEEL did not have a freeze/thaw chamber when testing began. The coupons were 3 inches wide and 11 inches long. For each coating type, as well as the uncoated samples, two coupon thicknesses (nominally 0.75 and 1.6 in.) were provided.

The freeze/thaw chamber was operated continuously, with the temperature varying from 0 to 40°F when thawing and 40 to 0°F when freezing. A thermocouple inserted in the thicker uncoated composite coupon was used to monitor specimen temperature (no evaluations were performed on this coupon), and thereby determine when to end a cycle. The coupons were subjected to 300 cycles. The composite coupons responded differently than do concrete coupons for which ASTM C666-92 was developed. Concrete coupons normally see 5 to 6 cycles per day with the cool down and warm up portions of the cycle requiring two hours each. Composite coupons could only be cycled between 3.5 and 4.5 times per day; the cool down portion required 1 hour while the warm up portion required 3 to 4 hours.

Another measure of coupon durability in freeze/thaw cycling is the relative dynamic modulus of elasticity, P_c .

$$P_c = (n_1^2/n^2) \times 100 \quad (1)$$

where

P_c = relative dynamic modulus of elasticity, after c cycles of freezing and thawing, in percent

n = fundamental transverse frequency at 0 cycles of freezing and thawing

n_1 = fundamental transverse frequency after c cycles of freezing and thawing.

If internal degradation occurs during testing, a drop in frequency is observed. When a concrete coupon reaches 60% of the initial modulus prior to 300 cycles, the testing is terminated. The value of n is 1.78 kHz at 3.5 cycles for the composite samples. Composite coupons experienced no drop in frequency after 300 cycles, indicating no internal degradation of the PMC occurred. No significant weight changes during freeze/thaw testing were observed. These results are consistent with weight changes observed in coupons exposed to QUV and Q-Fog testing. Based on the test reports from Construction Technology Laboratories, the composite coupons are freeze-thaw durable.

3.3 Fasteners

Fasteners were tested initially in two configurations, as individual bolts, washers, and nuts and as bolt assemblies torqued to 40 ft/lbs.^c in composite material. The bolting materials—plain finish carbon steel (A325), 316 stainless steel, hot dipped galvanized carbon steel (A325), and carbon steel (A325) with PCI-3^d corrosion-resistant finish—were exposed to salt spray, temperature cycling, and wet/dry cycling using the Q-Fog Cyclic Corrosion Tester in accordance with General Motors Engineering Standard GM9540, Method B, *Accelerated Corrosion Test*.⁶ Prior to accelerated aging, bolting specimens were weighed and measured; their surface areas were calculated. Bolting was exposed in the Q-Fog chamber for 2016 h. Specimens were repositioned weekly, i.e., the specimens next to the nozzle were moved away from the nozzle and those located in the outer areas were moved inwards. Specimens were examined for rusting (ASTM D610-95¹⁸), blistering (ASTM D714-94¹⁵), cracking (ASTM D661-93¹⁴), or any other surface anomalies (ASTM D662-93,¹⁹ ASTM D1654-92,²⁰ and ASTM D3274-95²¹). If visual examination revealed changes in bolting conditions between two cycles, photographs of the specimen were taken. Photographs were taken prior to any handling or quantitative measurement of the specimens. After 2016 h, the specimens were cleaned according to ASTM G1-90, *Standard Practice for Preparing, Cleaning, and Evaluating Corrosion*

c. The torque specified for assembling the bridge at INEEL.

d. Lone Star Proprietary Finish.

Test Specimens,²² and a weight loss and corrosion rate, if appropriate, were calculated. For each cleaning procedure, a blank was cleaned and a weight loss was calculated. The blank consisted of a fastener assembly (bolt, nut, and washer). This assembly was not exposed to test conditions, just cleaning procedures. Selected corroded bolt assemblies were examined by metallography.

In a one-way ANOVA, the analysis amounts to a formal comparison of mean outcomes on the dependent variables among the different levels of the treatment variables. For the bolt assembly data, this involves comparing the mean weight loss (corrosion) between the four different fastener types to see if there is any significant difference. Because there is random variability in the corrosion measured on individual bolt assemblies, even among those of the same type, some differences between the means can be expected simply due to chance. The ANOVA is used to determine whether or not the observed differences are big enough (compared to the random variability) to suggest that there is in fact a difference among them. The likelihood that the difference is due to chance is determined by calculating an F-statistic and an associated probability or p-value. The lower the p-value, the less likely that the observed differences would have occurred solely due to random differences. If the p-value for the corrosion data is less than 0.05 (on a probability scale from 0 to 1), the difference between fastener types is statistically significant, i.e. there is a real difference in the amount of corrosion.

The basic measure of corrosion for the four types of bolts assessed in the study was weight loss. In the case of plain, hot-dipped galvanized and PCI-3 finishes, the weight loss was corrected for the effects of the cleaning process by subtracting the weight loss for a control or blank bolt of the same finish. (The control bolts were not subjected to salt spray exposure but were cleaned using the same method used to clean the corresponding exposed bolts.) The weight loss data for the stainless steel bolts were not corrected for cleaning effects because the correction produced negative weight loss in three of the four bolts tested, indicating that such a correction was not generally necessary. After correction for the effects of cleaning, the weight loss values were converted to a weight loss rate measure (g/hr) by dividing by the number of hours of exposure to salt spray.

The weight loss rates are plotted in Figure 2. Individual values for each bolt type are plotted as open circles, mean values are plotted as smaller filled circles. Because the results differ by several orders of magnitude, the weight loss rates are plotted on a logarithmic scale.

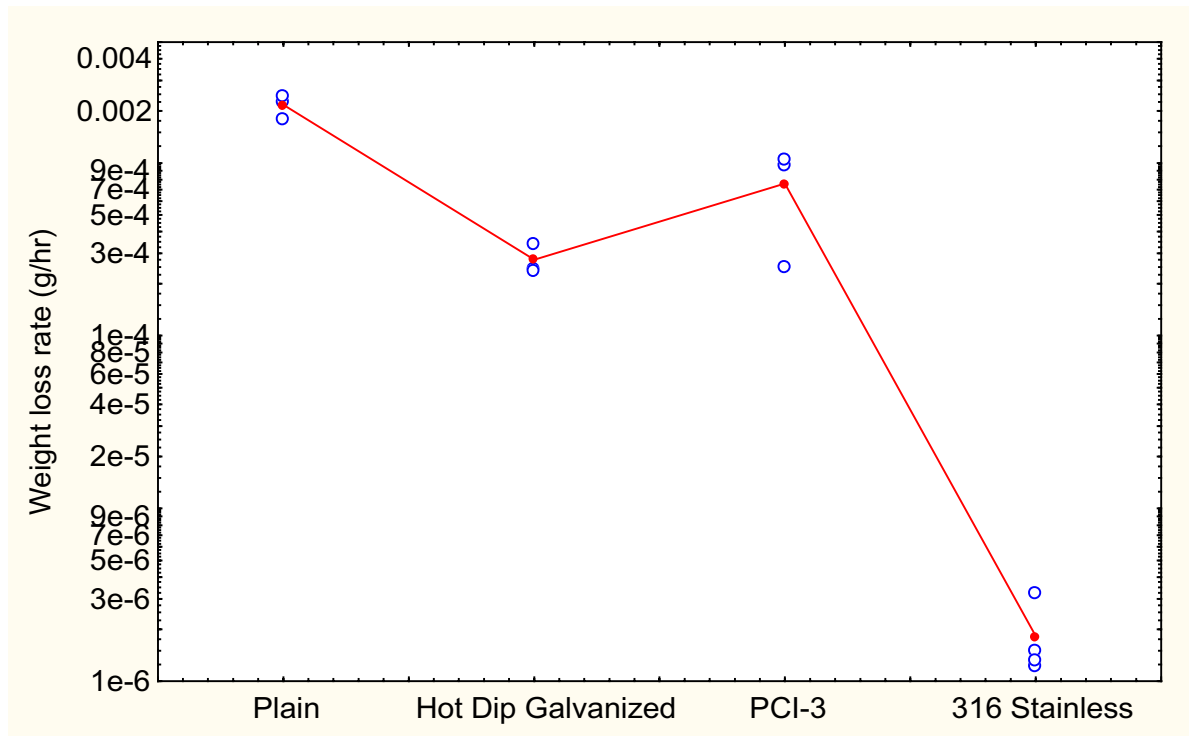


Figure 2. Plot of weight loss data by bolt type. (Note: two overlapping points exist at the lower value for the hot-dipped galvanized bolts and at the upper value for plain bolts.)

The data in Figure 2 show that the least amount of corrosion, by far, was suffered by the 316 stainless steel bolts. Plain bolts showed the most corrosion, while hot-dipped galvanized and PCI-3 coated bolts performed approximately the same. A one-way analysis of variance on the results confirmed that there were significant differences among the bolt types. The overall F test for the analysis of variance was highly significant ($F = 160$, $p = 0.0000$) while a subsequent test of paired differences showed highly significant results except for the comparison of hot-dipped galvanized and PCI-3 coatings, which was at best marginally significant. The paired differences confirm that the stainless steel bolts experienced by far the least corrosion; mean corrosion rates for the other bolt types were from 220 to 1200 times that for stainless steel. Differences in rates for the other three bolt types were not as great, approaching a factor of eight for plain vs. hot-dipped galvanized-coated bolts.

Note that the initial bolt material selections are nonstandard for load-bearing joints, rather A325 is used in slip-critical applications in steel bridge fabrication.²³ A second series of tests will be conducted to evaluate more appropriate materials for load-bearing joints in PMC bridges. The test plan will couple accelerated aging and mechanical testing. The goal of this test series is to provide research-based rank ordering of candidate fastener materials and to better establish cost/benefit measures for use in life-cycle cost planning by factoring in both degradation rates and loss of mechanical properties due to degradation.

4. CONCLUSIONS

Sensor and durability data for the PMC bridge indicate that the bridge design is suitable for use in the transportation infrastructure. Due to their ease of transport and installation, PMC bridges have the potential to provide rapidly deployable replacement bridges or bridge decks following natural disasters, such as floods, when existing abutments are structurally sound. PMC can be used in deck replacement situations as the installation process can be completed more quickly than with conventional methods, resulting in less traffic disruption. PMC decks also reduce the total weight of the bridge, allowing the same or increased load limits on the bridge.

Additional materials research on durability will be required to establish standards and guidelines to ensure prudent use of novel materials in the infrastructure as well as evaluate additional interaction effects such as water erosion and alkali attack. Fabrication steps, such as correct application of the UV coating, are critical and this UV coating durability research can provide guidance in developing research-based accelerated aging test plan protocols for evaluating composite materials for highway and other infrastructure applications. Additional sensor data are required to monitor in-service bridge performance as the PMC material ages. Accelerated aging research conducted using a statistically-based test matrix can provide data to rank candidate materials based on the interaction of environmental effects. Fastener material selection criteria should consider corrosion resistance and mechanical properties for load-bearing applications with PMC material as bolt replacement can be problematic if metal degradation occurs during service. Nondestructive evaluation techniques are required to inspect PMC structures. Selection of appropriate NDE techniques requires research data on failure mechanisms. Additional sensor, durability, and mechanical properties data are required to allow realistic life-cycle cost analysis.

5. ACKNOWLEDGEMENT

The authors recognize the contributions of Treasure Reho in collecting durability data and the technical advice of Ronald Mizia and Brad Norby. The accelerated aging research was funded through the INEEL's Long Term Research Initiative under DOE Idaho Operations Contract DE-AC07-94ID13223.

6. REFERENCES

1. M. A. Ehlen and H. E. Marshall, The Economics of New-Technology Materials: A Case Study of FRP Bridge Decking, NISTIR 5864, July 1996.
2. J. G. Rodriguez, N. M. Carlson, and S. A. Jensen, *INEEL Composite Bridge Testing Status Report*, INEEL/EXT-98-00425, June 1998.
3. W. D. Ketola and D. M. Grossman, (eds.), *Accelerated and Outdoor Durability Testing of Organic Materials* (STP 1202), American Society for Testing and Materials, 1994.
4. ASTM G53-95, *Standard Practice for Operating Light- and-Water Exposure Apparatus for Exposure of Nonmetallic Materials*, March 1995.

5. D. M. Grossman, "More Realistic Tests for Atmospheric Corrosion," *ASTM Standardization News*, April 1996, p. 34–39.
6. General Motors Engineering Standard GM9540-91, Method B, *Accelerated Corrosion Test*, July 1991.
7. ASTM D3170-87, *Standard Test Method for Chipping Resistance of Coatings*, July 1987.
8. ASTM D523-94, *Standard Test Method for Specular Gloss*, October 1994.
9. ASTM D2244-93, *Standard Test Method for Calculation of Color Differences from Instrumentally Measured Color Coordinates*, November 1993.
10. ASTM G147-96, *Conditioning and Handling of Nonmetallic Materials for Natural and Artificial Weathering Tests*, April 1997.
11. ASTM D5894-96, *Standard Practice for Cyclic Salt Fog/UV Exposure of Painted Metal, (Alternating Exposures in a Fog/Dry Cabinet and UV/Condensation Cabinet)*, March 1996.
12. ASTM D4214-89, *Standard Test Methods for Evaluating the Degree of Chalking of Exterior Paint Films*, June 1989.
13. ASTM D660-93, *Standard Test Method for Evaluating the Degree of Checking of Exterior Paints*, July 1993.
14. ASTM D661-93, *Standard Test Method for Evaluating the Degree of Cracking of Exterior Paints*, July 1993.
15. ASTM D714-94, *Standard Method for Evaluating the Degree of Blistering of Paints*, October 1994.
16. ASTM D772-86, *Standard Method for Evaluating the Degree of Flaking of Paints*, October 1986.
17. L. S. Crump, "Evaluating the Durability of Gel Coats Using Outdoor and Accelerated Weathering Techniques: A Correlation Study," *1996 Society of the Plastics Industry 51st Annual Conference*.
18. ASTM D610-95, *Standard Test Method for Evaluating the Degree of Rusting on Painted Steel Surfaces*, November 1995.
19. ASTM D662-93, *Standard Test Method for Evaluating Degree of Erosion of Exterior Paints*, July 1993.
20. ASTM D1654-92, *Standard Method for Evaluation of Painted or Coated Specimens Subjected to Corrosive Environments*, December 1992.
21. ASTM D3274-95, *Standard Test Method for Evaluating Degree of Surface Disfigurement of Paint Films by Microbial Growth or Soil and Dirt Accumulation*, June 1995.
22. ASTM G1-90, *Standard Practice for Preparing, Cleaning, And Evaluating Corrosion Test Specimens*, May 1990.
23. G. L. Kulak, J. W. Fisher, and J. H. Struik, *Guide to Design Criteria for Bolted and Riveted Joints*, John Wiley and Sons, 1987.